

**\*\*Volume Title\*\***  
**ASP Conference Series, Vol. \*\*Volume Number\*\***  
**\*\*Author\*\***  
 © **\*\*Copyright Year\*\*** Astronomical Society of the Pacific

## The role of quantum interference and partial redistribution in the solar Ba II D<sub>2</sub> 4554 Å line

H. N. Smitha<sup>1</sup>, K. N. Nagendra<sup>1</sup>, J. O. Stenflo<sup>2,3</sup> and M. Sampoorna<sup>1</sup>

<sup>1</sup>*Indian Institute of Astrophysics, Koramangala, Bengaluru, India*

<sup>2</sup>*Institute of Astronomy, ETH Zurich, CH-8093 Zurich, Switzerland*

<sup>3</sup>*Istituto Ricerche Solari Locarno, Via Patocchi, 6605 Locarno-Monti, Switzerland*

**Abstract.** The Ba II D<sub>2</sub> line at 4554 Å is a good example, where the  $F$ -state interference effects due to the odd isotopes produce polarization profiles, which are very different from those of the even isotopes that do not exhibit  $F$ -state interference. It is therefore necessary to account for the contributions from the different isotopes to understand the observed linear polarization profiles of this line. In this paper we present radiative transfer modeling with partial frequency redistribution (PRD), which is shown to be essential to model this line. This is because complete frequency redistribution (CRD) cannot reproduce the observed wing polarization. We present the observed and computed  $Q/I$  profiles at different limb distances. The theoretical profiles strongly depend on limb distance ( $\mu$ ) and the model atmosphere which fits the limb observations fails at other  $\mu$  positions.

### 1. Introduction

The interpretation of the Second Solar Spectrum requires taking into account a number of physical processes that are not relevant for the intensity spectrum. Some of the lines observed in the Second Solar Spectrum, like the Na I D<sub>1</sub> and D<sub>2</sub>, Cr I triplet at 5206 Å, Ba II D<sub>1</sub> and D<sub>2</sub>, Mg II h and k, and Ca II H and K, are affected by quantum interference between states of different total angular momentum ( $J$  or  $F$  states). The importance of quantum interference was first demonstrated both observationally and theoretically by Stenflo (1980, see also Stenflo 1997). An approximate theoretical approach for treating  $J$ -state interference with partial frequency redistribution (PRD) was proposed by Smitha et al. (2011, 2013a). This theory was then applied to model the linear polarization profiles of the Cr I triplet at 5204-5208 Å by Smitha et al. (2012a).

An atom with a nuclear spin  $I_s$  exhibits hyperfine structure splitting (HFS). The quantum interference between these hyperfine structure ( $F$ ) states produces depolarization in the line core. Na I D<sub>2</sub>, Ba II D<sub>2</sub>, and Sc II line at 4247 Å are some examples of spectral lines whose linear polarization profiles show signatures of  $F$ -state interference. The Ba II D<sub>2</sub> line is due to the transition from the upper  $J = 3/2$  and the lower  $J = 1/2$  fine structure levels (see Figure 1(a)). In the odd isotopes of Ba, both the upper and lower levels undergo HFS due to the nuclear spin  $I_s = 3/2$ . This gives rise to four upper and two lower  $F$ -states (see Figure 1(b)). In modeling the Ba II D<sub>2</sub> line it

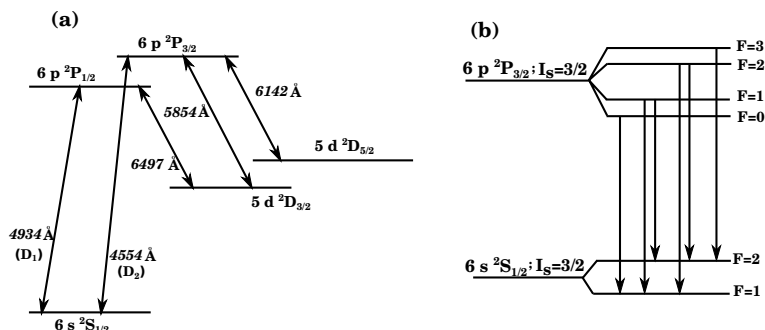


Figure 1. (a) the Ba II model atom for the even isotopes. For the odd isotopes the atomic model is modified by replacing two of the levels,  ${}^2P_{3/2}$  and  ${}^2S_{1/2}$ , with their hyperfine structure components (b). The energy levels are not drawn to the scale.

is necessary to account for quantum interference between the upper  $F$ -states. The odd isotopes constitute about 18% of the total Ba abundance in the Sun (c.f. Table 3 of Asplund et al. 2009). The rest 82% is from the even isotopes, which are not subject to HFS (because  $I_s = 0$ ).

High precision spectro-polarimetric observations by Stenflo & Keller (1997) using ZIMPOL clearly revealed the existence of three distinct peaks in the linear polarization ( $Q/I$ ) profiles of the Ba II  $D_2$  line. Using the last scattering approximation, Stenflo (1997) explained the physical origin of these three peaks. He showed that the central  $Q/I$  peak arises from the even isotopes of Ba, and the two side peaks from the odd isotopes. With a similar last scattering approach, the magnetic sensitivity of the Ba line was explored by Belluzzi et al. (2007). The above mentioned authors however did not account for radiative transfer and PRD effects. These effects were taken into account by Faurobert et al. (2009), but the treatment was limited to the even isotopes of Ba, for which HFS is absent. In Smitha et al. (2013b) we considered radiative transfer with PRD in both even and odd isotopes, and the full effects of HFS with  $F$ -state interferences. Here we present a brief summary of our attempts to model the Ba II  $D_2$  line profile observed in a quiet region close to the solar limb. Further we present center-to-limb variation (CLV) observations of this line and our initial attempts to model the same.

The paper is organized as follows: In Section 2 we present the polarized radiative transfer equation suitable to handle several isotopes of Ba simultaneously. In Section 3 we present the details of the observations. In Section 4 we discuss the model atom and the model atmosphere used. The results are presented in Section 5 with concluding remarks in Section 6.

## 2. Transfer equation for the Ba II $D_2$ case

The polarized transfer equation in a 1-D non-magnetic axisymmetric atmosphere is given by

$$\mu \frac{\partial \mathcal{I}(\lambda, \mu, z)}{\partial z} = -k_{\text{tot}}(\lambda, z) [\mathcal{I}(\lambda, \mu, z) - \mathcal{S}(\lambda, z)], \quad (1)$$

in the reduced Stokes vector basis (see Smitha et al. 2012a). Positive  $Q$  represents the linear polarization oriented parallel to the solar limb. The total opacity  $k_{\text{tot}}(\lambda, z) = k_l(z)\phi_g(\lambda, z) + \sigma_c(\lambda, z) + k_{\text{th}}(\lambda, z)$ , with  $\sigma_c$  and  $k_{\text{th}}$  being the continuum scattering and continuum absorption coefficients, respectively and  $k_l$  being the wavelength averaged absorption coefficient for the  $J_a \rightarrow J_b$  transition. Here  $J_a$  and  $J_b$  are the lower and upper level electronic angular momentum quantum numbers respectively. For the case of Ba II D<sub>2</sub>, the appropriate expression for the profile function  $\phi_g$  is

$$\phi_g(\lambda, z) = 0.822 \phi_e(\lambda, z) + 0.178 \phi_o(\lambda, z). \quad (2)$$

Here the Voigt profile function for the even isotopes of Ba II is denoted as  $\phi_e(\lambda, z)$ . This corresponds to the  $J_a = 1/2 \rightarrow J_b = 3/2$  transition in the absence of HFS.  $\phi_o(\lambda, z)$  is the profile function for the odd isotopes. It is the weighted sum of individual Voigt profiles  $\phi(\lambda_{F_b F_a}, z)$  representing each of the  $F_a \rightarrow F_b$  absorption transition. The initial and the intermediate hyperfine split levels have total angular momentum quantum numbers  $F_a$  and  $F_b$  respectively.  $\phi_o(\lambda, z)$  is given by

$$\begin{aligned} \phi_o(\lambda, z) = & \left[ \frac{2}{32}\phi(\lambda_{01}, z) + \frac{5}{32}\phi(\lambda_{11}, z) + \frac{5}{32}\phi(\lambda_{21}, z) \right. \\ & \left. + \frac{1}{32}\phi(\lambda_{12}, z) + \frac{5}{32}\phi(\lambda_{22}, z) + \frac{14}{32}\phi(\lambda_{32}, z) \right]. \end{aligned} \quad (3)$$

In Equation (2) the contributions from both the <sup>135</sup>Ba (6.6%) and <sup>137</sup>Ba (11.2%) odd isotopes add upto the 17.8% of  $\phi_o(\lambda, z)$ . In Equation (1),  $\mathcal{S}(\lambda, z)$  is the reduced total source vector for a two-level atom with an unpolarized lower level and is defined as

$$\begin{aligned} \mathcal{S}(\lambda, z) = & \frac{k_l(z)\mathcal{S}_l(\lambda, z) + \sigma_c(\lambda, z)\mathcal{S}_c(\lambda, z) + k_{\text{th}}(\lambda, z)\mathcal{S}_{\text{th}}(\lambda, z)}{k_{\text{tot}}(\lambda, z)} \\ & + \frac{\epsilon k_l(z)\phi_g(\lambda, z)\mathcal{S}_{\text{th}}(\lambda, z)}{k_{\text{tot}}(\lambda, z)}. \end{aligned} \quad (4)$$

Derouich (2008) showed that, for the case of Ba II D<sub>2</sub> any ground level polarization would be destroyed by elastic collisions with hydrogen atoms (see also Faurobert et al. 2009).

In Equation (4),  $\mathcal{S}_{\text{th}} = (B_\lambda, 0)^T$ , where  $B_\lambda$  is the Planck function. The line source vector  $\mathcal{S}_l(\lambda, z)$  is

$$\mathcal{S}_l(\lambda, z) = \int_0^{+\infty} \frac{1}{2} \int_{-1}^{+1} \widetilde{\mathcal{R}}(\lambda, \lambda', z) \hat{\Psi}(\mu') \mathcal{I}(\lambda', \mu', z) d\mu' d\lambda', \quad (5)$$

with

$$\widetilde{\mathcal{R}}(\lambda, \lambda', z) = 0.822 \widetilde{\mathcal{R}}_e(\lambda, \lambda', z) + 0.178 \widetilde{\mathcal{R}}_o(\lambda, \lambda', z). \quad (6)$$

Here  $\widetilde{\mathcal{R}}_o(\lambda, \lambda', z)$  is a  $(2 \times 2)$  diagonal matrix, including the effects of HFS in odd isotopes.  $\widetilde{\mathcal{R}}_o = \text{diag}(\mathcal{R}_o^0, \mathcal{R}_o^2)$ , with  $\mathcal{R}_o^K$  being the redistribution function components for the multipolar index  $K$ , containing both type-II and type-III redistribution of Hummer (1962). The quantum number replacement  $L \rightarrow J$ ;  $J \rightarrow F$ ;  $S \rightarrow I_s$  in Equation (7) of Smitha et al. (2012a, see also Smitha et al. 2012b and Smitha et al. 2013a) gives the expression for  $\mathcal{R}^K$ . We use CRD functions in place of the type-III redistribution functions as in Smitha et al. (2013b). The contributions from the individual redistribution matrices for the odd isotopes <sup>135</sup>Ba and <sup>137</sup>Ba are also taken into account.

$\widetilde{\mathcal{R}}_e(\lambda, \lambda', z)$  is also a  $(2 \times 2)$  diagonal matrix for the even isotopes without HFS. Its elements  $\mathcal{R}_e^K$  are the redistribution functions corresponding to the scattering transition  $J_a = 1/2 \rightarrow J_b = 3/2 \rightarrow J_f = 1/2$ . They are obtained by setting the nuclear spin  $I_s = 0$  in  $\widetilde{\mathcal{R}}_o(\lambda, \lambda', z)$ . An expression for  $\widetilde{\mathcal{R}}_e(\lambda, \lambda', z)$  in the Stokes vector basis can be found in Domke & Hubeny (1988) and in Bommier (1997, see also Nagendra 1994, Sampoorna 2011).

We here use the angle-averaged versions of these quantities. Supriya et al. (2013) showed that in the non-magnetic case the use of the angle-averaged redistribution matrix is sufficiently accurate for all practical purposes.

We use the two branching ratios (see Smitha et al. 2012b, 2013b)

$$A = \frac{\Gamma_R}{\Gamma_R + \Gamma_I + \Gamma_E}, \quad B^{(K)} = \frac{\Gamma_R}{\Gamma_R + \Gamma_I + D^{(K)}} \frac{\Gamma_E - D^{(K)}}{\Gamma_R + \Gamma_I + \Gamma_E}, \quad (7)$$

where  $\Gamma_R$  and  $\Gamma_I$  are the radiative and inelastic collisional rates, respectively.  $\Gamma_E$  is the elastic collision rate computed from Barklem & O'Mara (1998). The depolarizing elastic collision rates are given by  $D^{(K)}$  with  $D^{(0)} = 0$ . The  $D^{(2)}$  is computed using (see Derouich 2008; Faurobert et al. 2009)

$$D^{(2)} = 6.82 \times 10^{-9} n_H (T/5000)^{0.40} + 7.44 \times 10^{-9} (1/2)^{1.5} n_H (T/5000)^{0.38} \exp(\Delta E/kT), \quad (8)$$

where  $n_H$  is the neutral hydrogen number density in  $(\text{cm}^{-3})$ ,  $T$  the temperature in kelvin, and  $\Delta E$  the energy difference between the  $^2P_{1/2}$  and  $^2P_{3/2}$  fine structure levels in  $(\text{cm}^{-1})$  and  $k$  is the Boltzmann constant in  $(\text{cm}^{-1}/\text{K})$ . We neglect the collisional coupling between the  $^2P_{3/2}$  level and the metastable  $^2D_{5/2}$  level (see Smitha et al. 2013b). Derouich (2008) pointed out the importance of  $^2P_{3/2} - ^2D_{5/2}$  collisions for the line center polarization of Ba II  $D_2$ . He showed that the neglect of such collisions would lead to an overestimate of the line core polarization by  $\sim 25\%$ . It was shown by Faurobert et al. (2009) that this in turn would lead to an overestimate of the microturbulent magnetic field ( $B_{\text{turb}}$ ) by  $\sim 35\%$ . Our aim is to explore the roles of PRD, HFS, quantum interferences, and the atmospheric temperature structure in the modeling of the triple peak structure of the Ba II  $D_2$  linear polarization profile.

We assume frequency coherent scattering in the continuum (see Smitha et al. 2012a) with its source vector given by

$$\mathcal{S}_c(\lambda, z) = \frac{1}{2} \int_{-1}^{+1} \hat{\Psi}(\mu') \mathcal{I}(\lambda, \mu', z) d\mu'. \quad (9)$$

The matrix  $\hat{\Psi}$  is the Rayleigh scattering phase matrix in the reduced basis (see Frisch 2007).  $\epsilon$  is the line thermalization parameter defined by  $\epsilon = \Gamma_I/(\Gamma_R + \Gamma_I)$ . The Stokes vector  $(I, Q)^T$  can be computed from the irreducible Stokes vector  $\mathcal{I}$  by simple transformations (see Frisch 2007).

### 3. Observations

The observed polarization profiles of the Ba II  $D_2$  line shown in this paper for  $\mu = 0.1$  are same as those presented in Smitha et al. (2013b). The observations for all  $\mu$  values were

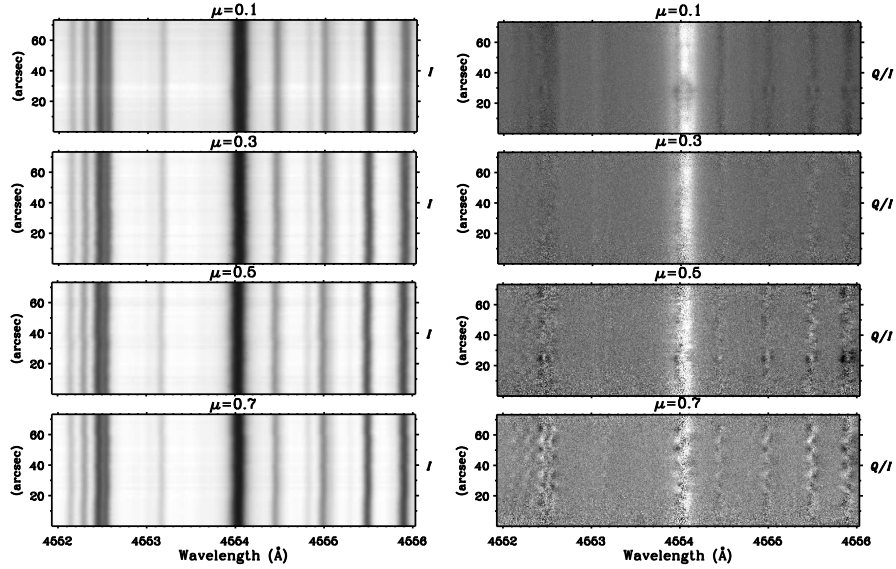


Figure 2. CCD images of  $I$  and  $Q/I$  observed at different limb distances on the solar disk.

acquired by the ETH team of Stenflo on June 3, 2008, using their ZIMPOL-2 imaging polarimetry system (Gandorfer et al. 2004) at the THEMIS telescope on Tenerife. The polarization modulation was done using Ferroelectric Liquid Crystal modulators. The observations were recorded at various limb distances with the slit being placed parallel to the heliographic north pole. Figure 2 shows the CCD images of  $I$  and  $Q/I$  for different  $\mu$  values. These essentially represent the CLV of the intensity and degree of linear polarization. In the Section 5 we attempt to model these CLV observations.

#### 4. Model atom and model atmosphere

The observed ( $I$ ,  $Q/I$ ) profiles of the Ba II D<sub>2</sub> line can be modeled using a two-stage process. This process is similar to the one described in Holzreuter et al. (2005, see also Anusha et al. 2010, 2011, Smitha et al. 2012a, 2013b). In this two-stage process, the intensity is first computed which is then used as an input to compute the polarization. The code that is used for computing the intensity was developed by Uitenbroek (2001, referred to as the RH-code). To compute the intensity and polarization we need a model atom that is representative of the atom under consideration and a one-dimensional model atmosphere that mimics the solar atmosphere. For the case of Ba II D<sub>2</sub>, since the effects of different isotopes are to be taken into account, we construct three different atom models. Out of these, two are for the odd and one for the even isotope. The atom model for the even isotope (<sup>138</sup>Ba) is given by the five levels of Figure 1(a), while for the odd isotopes (<sup>135</sup>Ba and <sup>137</sup>Ba) the model is extended to include the hyperfine splitting as described by Figure 1(b). The HFS of the <sup>2</sup>P<sub>1/2</sub> level and the metastable levels are neglected. The effects of HFS are taken into account only for the D<sub>2</sub> transition in the intensity computations. For the odd isotopes, the radiative transitions between <sup>2</sup>P<sub>3/2</sub>

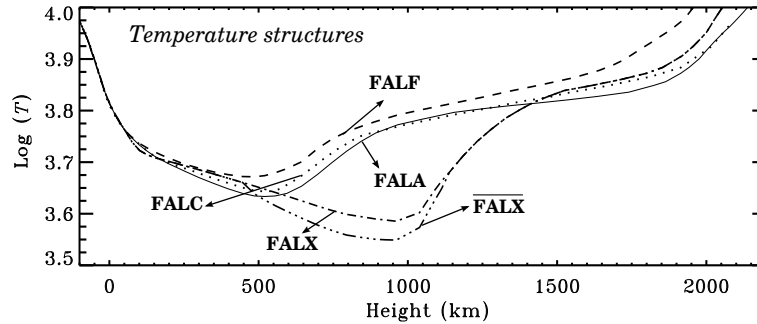


Figure 3. The temperature structures of the standard FALA, FALC, FALF, FALX, and the modified  $\overline{\text{FALX}}$  model atmospheres.

and the metastable levels are treated in the same way as for the even isotope. However, in the polarization computations, under the two-level atom approximation, the coupling to the metastable levels are neglected for both even and odd isotopes. We neglect the contribution from other less abundant even isotopes. The wavelengths of the six hyperfine transitions for the odd isotopes are taken from Kurucz' database and are also listed in Table 1 of Smitha et al. (2013b). The line strengths of these transitions are given in Equation (3).

Some of the commonly used standard 1-D solar model atmospheres are the FALA, FALF, FALC (see Fontenla et al. 1993) and the FALX (see Avrett 1995). Among these four models FALF is the hottest and FALX the coolest. However, as will be discussed below, we find that a model atmosphere that is cooler than FALX is needed to fit the observed profiles. The new model, denoted  $\overline{\text{FALX}}$ , is obtained by reducing the temperature of the FALX model by about 300 K in the height range 500 – 1200 km above the photosphere. The temperature structures of the standard model atmospheres and the modified model are shown in Figure 3.

## 5. Results

### 5.1. Modeling the limb observations

The three atom models of Ba II atom described in the above section give us three different sets of physical quantities (two for the odd isotopes and one for the even isotope) when used in the RH code to compute intensity. These quantities are the line opacity, line emissivity, continuum absorption coefficient, continuum emissivity, continuum scattering coefficient, and the mean intensity. See Uitenbroek (2001) for the mathematical expressions that are used in the RH-code to compute these quantities for the even isotopes. For the odd isotopes, the profile functions in these expressions are replaced by  $\phi_o(\lambda, z)$  defined by Equation (3).

The three sets of quantities obtained from three atom models are combined in the ratio of their respective isotope abundances. The combined quantities are then used as inputs to the polarization code. The  $Q/I$  profiles so computed for the various model atmospheres are shown in Figure 4. The figure shows that the  $Q/I$  profiles are quite sensitive to the temperature structure of the model atmosphere and that the central peak

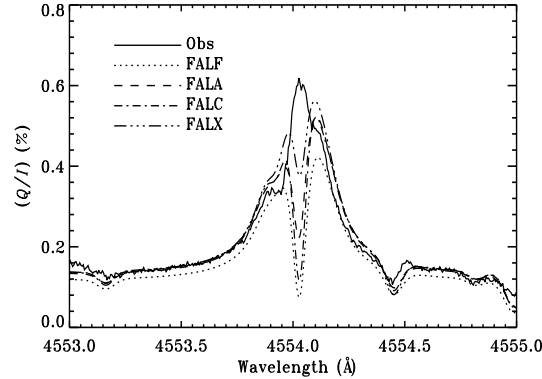


Figure 4. Comparison between the observed and theoretical  $Q/I$  profiles computed using different model atmospheres.

cannot be reproduced from any of the standard model atmospheres. All the models produce a dip in  $Q/I$  at the line center. Earlier studies have shown that such a central dip in  $Q/I$  is generally due to the effects of PRD (see for example, Figure 3 of Faurobert-Scholl 1992, and Figure 6 of Holzreuter et al. 2005). The main contribution to this dip comes from the type-II frequency redistribution. In the case of Ba II  $D_2$ , the central dip is formed mainly through contributions from the even isotopes (see Figure 5 of Smitha et al. 2013b). However the profiles computed using only CRD do not show any central dip. It is generally known that  $Q/I$  profiles computed with CRD and PRD in realistic model atmospheres differ not only in the line wings but also in the line core (see for e.g., Faurobert-Scholl 1992; Holzreuter et al. 2005; Faurobert et al. 2009; Smitha et al. 2012a). This is contrary to the behaviour expected of  $Q/I$  profiles computed in isothermal atmospheres, where they nearly match. A study of the mechanisms that cause the differences in the line core, in the case of realistic atmospheres, would be taken up in a forthcoming publication.

Holzreuter et al. (2005) show that the magnitude of the  $Q/I$  central dip is strongly dependent on the choice of atmospheric parameters. The central dip becomes shallower for cooler models. This behavior is also evident from our Figure 4. Such dips in  $Q/I$  are common in line profile modeling with PRD, and are often smoothed out by applying instrumental and macro-turbulent broadening. The profiles presented in Figure 4 have already been smeared with a Gaussian function having a full width at half maximum (FWHM) of 70 mÅ. Though it is possible to smoothen out the dip by increasing the smearwidth, it will suppress the side peaks which are due to the odd isotopes and also disturbs the fit to the intensity profile. A smearwidth value of 70 mÅ has been chosen by us to optimize the fit and it is also consistent with what we expect based on the observing parameters and turbulence in the chromosphere.

Since all the standard model atmospheres failed to provide a fit, we had to modify the temperature structure of the FALX model to get a new much cooler model. This modified model is called the FALX and the details of its construction are given in Smitha et al. (2013b). This new model atmosphere succeeds in fitting both the intensity and the linear polarization profiles. The fit to the  $Q/I$  profile is shown as the dashed line in Figure 5. The theoretical profile in this figure also includes the contribution from the spectrograph stray light which is 4% of the continuum intensity. This is done to mimic

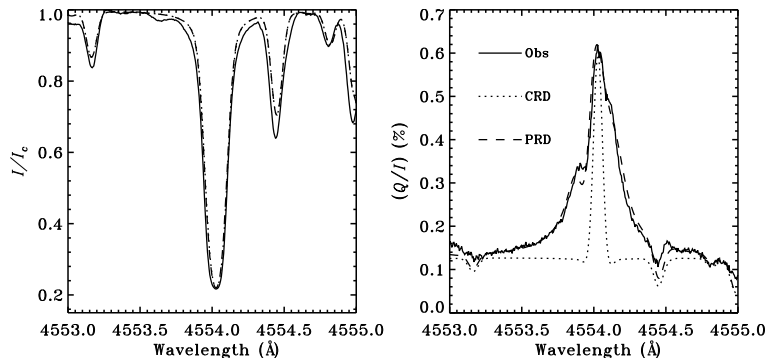


Figure 5. Fit to the observed  $Q/I$  profiles using the  $\overline{\text{FALX}}$  model atmosphere and also the comparison between profiles computed with PRD and CRD.

the observed profiles which contain the contribution from stray light. Finally, the effect of microturbulent magnetic field with a strength of 2 G is included to obtain a good  $Q/I$  fit at the line center.

The Ba II D<sub>2</sub> 4554 Å line is a resonance line and is strongly influenced by the effects of PRD. Hence it is very important to take account of the PRD effects while modeling. Its importance in case of the even isotopes of Ba II is demonstrated in Faurobert et al. (2009). In the right panel of Figure 5, we present a comparison between the observed and the theoretical  $Q/I$  profiles based on CRD alone (dotted line) and on full PRD (dashed line) for the  $\overline{\text{FALX}}$  model. The intensity profile can be fitted well using either PRD or CRD (see Smitha et al. 2013b), but the polarization profile cannot be fitted with CRD alone. This shows that the effects of PRD are essential to model the  $Q/I$  profiles of the Ba II D<sub>2</sub> line.

## 5.2. Modeling the CLV observations

The left panel of Figure 6 shows the CLV of the observed  $Q/I$  profiles. The right panel of this figure shows the CLV of the theoretical  $Q/I$  profiles computed using the  $\overline{\text{FALX}}$  model atmosphere. As seen from the right panel, the newly constructed model atmosphere, though successfully fits the observed profiles for  $\mu = 0.1$ , fails to fit the observations for  $\mu > 0.1$ . In fact for  $\mu > 0.1$ , we again obtain a central dip instead of a peak in the  $Q/I$  profiles. The central dip becomes deeper as  $\mu \rightarrow 1$ . This behavior was noticed also for the case of Na I D<sub>2</sub> by Holzreuter et al. (2005). Thus the modification in the temperature structure of the  $\overline{\text{FALX}}$  model atmosphere, presented in Smitha et al. (2013b) and in this paper, helps only for  $\mu = 0.1$ . For other  $\mu$  positions, the temperature structure has to be further modified. Thus we are unable to find a single 1D model atmosphere that fits the CLV observations of the Ba II D<sub>2</sub> line.<sup>1</sup>

<sup>1</sup>In fact the complexity of the problem is such that no single 1D model atmosphere fits the observations of different lines, apart from observations of the same line at different  $\mu$  positions. For example, when modeling the Cr I triplet in Smitha et al. (2012a), we had to modify the temperature structure of the  $\overline{\text{FALX}}$  model atmosphere in the deeper layers to obtain a fit to the  $(I, Q/I)$  observations at  $\mu = 0.15$ .



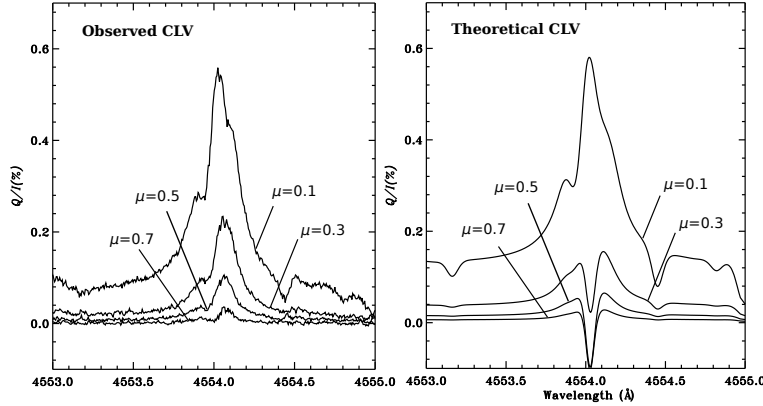


Figure 6. Comparison between the observed center to limb variation (CLV) of the  $Q/I$  profiles and the theoretically computed CLV. The theoretical profiles are computed using the FALX model atmosphere.

## 6. Conclusions

In this paper we briefly describe the results of our previous paper on modeling the polarization profiles of the Ba II D<sub>2</sub> line by taking full account of PRD, radiative transfer, and HFS effects. Also, we extend the same to model the observed CLV of the  $Q/I$  profiles. To model the CLV profiles, we use the same approach that was used in Smitha et al. (2013b). We find that some of the standard model atmospheres like the FALF, FALC, FALA, and FALX fail to reproduce the central peak, and instead give a central dip which is mainly due to PRD effects. Also, this central dip is quite sensitive to the temperature structure of the model atmosphere. By slightly modifying the temperature of the standard FALX model atmosphere, we obtain a fit to both  $I$  and  $Q/I$  profiles. This new model is called the  $\bar{\text{FALX}}$ . However this new model successfully fits the observations only for  $\mu = 0.1$  and fails at other limb distances. Hence within the sample of the model atmospheres tested by us, no single one dimensional, single component model atmosphere succeeds in reproducing the observed  $Q/I$  profiles at all limb distances. This possibly indicates that multi-dimensional transfer effects are required to model the CLV observations of this line.

Finally, we show that since the Ba II D<sub>2</sub> is a strong resonance line, it has damping wings that are governed by PRD. It is therefore necessary to take full account of PRD in order to correctly model the  $Q/I$  profile. In contrast, the intensity profiles computed with PRD or CRD do not differ substantially from each other through out the entire line profile.

**Acknowledgments.** We would like to thank Dr. Michele Bianda for useful discussions. We acknowledge the use of HYDRA cluster facility at the Indian Institute of Astrophysics for computing the results presented in the paper. We would like to thank the Referee for a careful reading of the manuscript and for giving useful comments and suggestions.

**References**

- Anusha, L. S., Nagendra, K. N., Bianda, M., Stenflo, J. O., Holzreuter, R., Sampoorna, M., Frisch, H., Ramelli, R., & Smitha, H. N. 2011, *ApJ*, 737, 95
- Anusha, L. S., Nagendra, K. N., Stenflo, J. O., Bianda, M., Sampoorna, M., Frisch, H., Holzreuter, R., & Ramelli, R. 2010, *ApJ*, 718, 988
- Asplund, M., Grevesse, N., Sauval, A. J., & Scott, P. 2009, *ARA&A*, 47, 481
- Avrett, E. H. 1995, in *Infrared tools for solar astrophysics: What's next?*, edited by J. R. Kuhn, & M. J. Penn, 303
- Barklem, P. S., & O'Mara, B. J. 1998, *MNRAS*, 300, 863
- Belluzzi, L., Trujillo Bueno, J., & Landi Degl'Innocenti, E. 2007, *ApJ*, 666, 588
- Bommier, V. 1997, *A&A*, 328, 706
- Derouich, M. 2008, *A&A*, 481, 845
- Domke, H., & Hubeny, I. 1988, *ApJ*, 334, 527
- Faurobert, M., Derouich, M., Bommier, V., & Arnaud, J. 2009, *A&A*, 493, 201
- Faurobert-Scholl, M. 1992, *A&A*, 258, 521
- Fontenla, J. M., Avrett, E. H., & Loeser, R. 1993, *ApJ*, 406, 319
- Frisch, H. 2007, *A&A*, 476, 665
- Gandorfer, A. M., Steiner, H. P. P., Aebbersold, F., Egger, U., Feller, A., Gisler, D., Hagenbuch, S., & Stenflo, J. O. 2004, *A&A*, 422, 703
- Holzreuter, R., Fluri, D. M., & Stenflo, J. O. 2005, *A&A*, 434, 713
- Hummer, D. G. 1962, *MNRAS*, 125, 21
- Nagendra, K. N. 1994, *ApJ*, 432, 274
- Sampoorna, M. 2011, *ApJ*, 731, 114
- Smitha, H. N., Nagendra, K. N., Sampoorna, M., & Stenflo, J. O. 2013a, *QSRT*, 115, 46
- Smitha, H. N., Nagendra, K. N., Stenflo, J. O., Bianda, M., Sampoorna, M., Ramelli, R., & Anusha, L. S. 2012a, *A&A*, 541, A24
- Smitha, H. N., Nagendra, K. N., Stenflo, J. O., & Sampoorna, M. 2013b, *ApJ*, 768, 163
- Smitha, H. N., Sampoorna, M., Nagendra, K. N., & Stenflo, J. O. 2011, *ApJ*, 733, 4
- Smitha, H. N., Sowmya, K., Nagendra, K. N., Sampoorna, M., & Stenflo, J. O. 2012b, *ApJ*, 758, 112
- Stenflo, J. O. 1980, *A&A*, 84, 68
- 1997, *A&A*, 324, 344
- Stenflo, J. O., & Keller, C. U. 1997, *A&A*, 321, 927
- Supriya, H. D., Smitha, H. N., Nagendra, K. N., Ravindra, B., & Sampoorna, M. 2013, *MNRAS*, 429, 275
- Uitenbroek, H. 2001, *ApJ*, 557, 389